

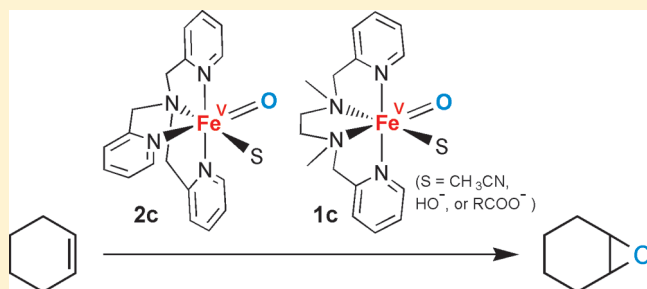
EPR, ^1H and ^2H NMR, and Reactivity Studies of the Iron–Oxygen Intermediates in Bioinspired Catalyst Systems

Oleg Y. Lyakin, Konstantin P. Bryliakov, and Evgenii P. Talsi*

Boreskov Institute of Catalysis, Siberian Branch of the Russian Academy of Sciences, Pr. Lavrentieva 5, Novosibirsk 630090, Russian Federation, and Novosibirsk State University, Ul. Pirogova 2, Novosibirsk 630090, Russian Federation

Supporting Information

ABSTRACT: Complexes $[(\text{BPMEN})\text{Fe}^{\text{II}}(\text{CH}_3\text{CN})_2](\text{ClO}_4)_2$ (**1**, BPMEN = *N,N'*-dimethyl-*N,N'*-bis(2-pyridylmethyl)-1,2-diaminoethane) and $[(\text{TPA})\text{Fe}^{\text{II}}(\text{CH}_3\text{CN})_2](\text{ClO}_4)_2$ (**2**, TPA = tris(2-pyridylmethyl)amine) are among the best nonheme iron-based catalysts for bioinspired oxidation of hydrocarbons. Using EPR and ^1H and ^2H NMR spectroscopy, the iron–oxygen intermediates formed in the catalyst systems **1,2**/ H_2O_2 ; **1,2**/ $\text{H}_2\text{O}_2/\text{CH}_3\text{COOH}$; **1,2**/ $\text{CH}_3\text{CO}_3\text{H}$; **1,2**/*m*-CPBA; **1,2**/ PhIO ; **1,2**/ $^t\text{BuOOH}$; and **1,2**/ $^t\text{BuOOH}/\text{CH}_3\text{COOH}$ have been studied (*m*-CPBA is *m*-chloroperbenzoic acid). The following intermediates have been observed: $[(\text{L})\text{Fe}^{\text{III}}(\text{OOR})(\text{S})]^{2+}$, $[(\text{L})\text{Fe}^{\text{IV}}=\text{O}(\text{S})]^{2+}$ (L = BPMEN or TPA, R = H or ^tBu , S = CH_3CN or H_2O), and the iron–oxygen species **1c** (L = BPMEN) and **2c** (L = TPA). It has been shown that **1c** and **2c** directly react with cyclohexene to yield cyclohexene oxide, whereas $[(\text{L})\text{Fe}^{\text{IV}}=\text{O}(\text{S})]^{2+}$ react with cyclohexene to yield mainly products of allylic oxidation. $[(\text{L})\text{Fe}^{\text{III}}(\text{OOR})(\text{S})]^{2+}$ are inert in this reaction. The analysis of EPR and reactivity data shows that only those catalyst systems which display EPR spectra of **1c** and **2c** are able to selectively epoxidize cyclohexene, thus bearing strong evidence in favor of the key role of **1c** and **2c** in selective epoxidation. **1c** and **2c** were tentatively assigned to the oxoiron(V) intermediates.



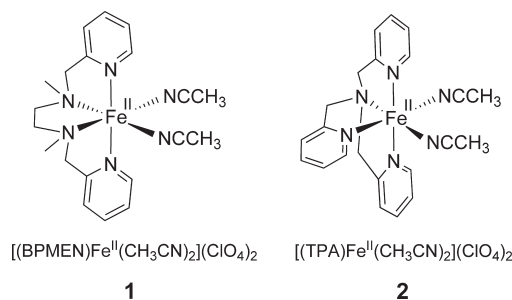
INTRODUCTION

The design of new iron-based catalyst systems which can selectively oxidize organic substrates is a challenging goal.^{1–27} Iron complexes with aminopyridine ligands $[(\text{BPMEN})\text{Fe}^{\text{II}}(\text{CH}_3\text{CN})_2](\text{ClO}_4)_2$ (**1**) and $[(\text{TPA})\text{Fe}^{\text{II}}(\text{CH}_3\text{CN})_2](\text{ClO}_4)_2$ (**2**) (Chart 1) are the most studied nonheme iron-based catalysts for selective alkene oxidation with H_2O_2 and $\text{CH}_3\text{CO}_3\text{H}$.^{2,5,8,10,11,28}

Two types of intermediates, such as iron(III) hydroperoxo complex $[(\text{L})\text{Fe}^{\text{III}}-\text{OOH}]^{2+}$ and oxoiron(IV) complex $[(\text{L})\text{Fe}^{\text{IV}}=\text{O}(\text{S})]^{2+}$ (L = BPMEN or TPA, S = CH_3CN or H_2O), have been observed in the catalyst systems **1,2**/ H_2O_2 and **1,2**/ $\text{CH}_3\text{CO}_3\text{H}$, respectively.^{11,27–33} However, the direct reactivity studies of $[(\text{L})\text{Fe}^{\text{III}}-\text{OOH}]^{2+}$ (L = BPMEN or TPA) have shown that those species are sluggish oxidants and cannot be themselves responsible for the selective oxidation of hydrocarbons.^{27,31,32,34} The independently determined selectivity of $[(\text{TPA})\text{Fe}^{\text{IV}}=\text{O}(\text{S})]^{2+}$ toward epoxidation of cyclooctene was also poor and could not explain the observed yield of epoxide in the catalyst system **1**/ $\text{CH}_3\text{CO}_3\text{H}/\text{cyclooctene}$.^{28,30} Hence, neither $[(\text{L})\text{Fe}^{\text{III}}-\text{OOH}]^{2+}$ nor $[(\text{L})\text{Fe}^{\text{IV}}=\text{O}(\text{S})]^{2+}$ species can drive the selective epoxidation of olefins by catalyst systems **1,2**/ H_2O_2 and **1,2**/ $\text{CH}_3\text{CO}_3\text{H}$. It was proposed recently that the actual active species are oxoiron(V) complexes $\text{LFe}^{\text{V}}=\text{O}$.²⁸

Although an oxoiron(V) intermediate $[(\text{TAML})\text{Fe}^{\text{V}}=\text{O}]^-$, where TAML is a macrocyclic tetraamide ligand, was synthesized

Chart 1. Complexes Studied Herein



and characterized by various spectroscopic techniques,³⁵ evidence for the involvement of oxoiron(V) species as active oxidants in catalytic oxygenation reactions was indirect and mainly came from product analysis and the incorporation of ^{18}O from H_2^{18}O into the products of isotopic labeling experiments.⁸ Therefore, it is very important to identify the actual active species of the catalyst systems **1,2**/ H_2O_2 ($\text{CH}_3\text{CO}_3\text{H}$). Recently, we reported on the EPR spectroscopic trapping of the new highly reactive iron–oxygen intermediates.³⁶

Received: January 14, 2011

Published: May 20, 2011

Direct reactivity studies have shown that these species are responsible for the selective epoxidation of cyclohexene by the $1/2/\text{CH}_3\text{CO}_3\text{H}$ and $1/\text{H}_2\text{O}_2$ systems. On the basis of the EPR and reactivity data, these species are proposed to be oxoiron(V) intermediates.³⁶

In this work, we present the results of the systematic EPR and ^1H and ^2H NMR spectroscopic studies of the iron–oxygen intermediates formed upon the interaction of complexes **1** and **2** with various oxidants: H_2O_2 , $\text{H}_2\text{O}_2/\text{CH}_3\text{COOH}$, $\text{CH}_3\text{CO}_3\text{H}$, *m*-CPBA, PhIO, $^t\text{BuOOH}$, and $^t\text{BuOOH}/\text{CH}_3\text{COOH}$.³⁷ On the basis of the observed reactivities of the intermediates toward selective epoxidation of cyclohexene, their role in selective epoxidation is discussed.

RESULTS AND DISCUSSION

EPR Characterization of the Intermediates Formed in the System $1/\text{H}_2\text{O}_2$. The starting complex **1** is EPR-silent. In order to observe the EPR spectra of the unstable intermediates in the system $1/\text{H}_2\text{O}_2$, we used a 1.7:1 $\text{CH}_2\text{Cl}_2/\text{CH}_3\text{CN}$ mixture as a solvent. The addition of CH_2Cl_2 allows lowering of the temperature of the reaction solution (down to $-70\text{ }^\circ\text{C}$) without freezing and provides more sharp resonances in the EPR spectra of frozen solutions ($-196\text{ }^\circ\text{C}$). The latter effect can be attributed to the formation of a better glass upon freezing. The solution of 95% H_2O_2 in a 1.7:1 $\text{CH}_2\text{Cl}_2/\text{CH}_3\text{CN}$ mixture was used as a source of H_2O_2 .

The EPR spectrum of the sample frozen 30 s after the addition of 2 equiv of H_2O_2 to the 0.027 M solution of **1** in a 1.7:1 $\text{CH}_2\text{Cl}_2/\text{CH}_3\text{CN}$ mixture at $-60\text{ }^\circ\text{C}$ displays resonances from the low-spin ($S = 1/2$) ferric species **1a** and **1b** (g values in the range 1.9–2.4) and the resonance at $g = 4.2$ from an unidentified high-spin ($S = 5/2$) ferric species (Figure 1A). Storing this sample for 5 min at $-70\text{ }^\circ\text{C}$ leads to a decrease of the concentration of **1b**, and resonances of a new complex **1c** appear (Figure 1B).

The EPR spectrum of the sample recorded 30 s after mixing **1** with 10 equiv of H_2O_2 at $-60\text{ }^\circ\text{C}$ predominantly displays resonances of complex **1b** (Figure 1C). Storing this sample for 5 min at $-70\text{ }^\circ\text{C}$ results in an increase of the concentration of complexes **1c** and **1a** (Figure 1D). It is worth noting that the ratio of **1a** and **1b** observed just after mixing the reagents at $-60\text{ }^\circ\text{C}$ can greatly change in attempts to reproduce one and the same sample, since it is difficult to precisely control the rapid mixing of the reagents at low temperatures. However, **1c** always appears after **1a** and **1b**.

Hence, three types of the low-spin iron species (**1a–c**) can be observed in the system $1/\text{H}_2\text{O}_2$ at low temperatures. **1a–c** display rhombic EPR spectra typical for $S = 1/2$ species. Some of the resonances of these species overlap. Fortunately, it is possible to find appropriate conditions, when the particular complex prevails and thus reliably assign its resonances (Figure 1B,C and Table 1). It is worth noting that the detection of the resonance of **1c** at $g_3 = 1.70$ is complicated by overlap with the very broad signal of unidentified ferric species at $g \approx 2$ with a peak-to-peak width of $\sim 1000\text{ G}$ (Figure 1B). The intensity of the latter signal grows with time. The variation of the $[\text{H}_2\text{O}_2]/[\mathbf{1}]$ ratio and the detection of the EPR spectra at the early stages after the reaction onset allow one to reliably observe the resonance at $g_3 = 1.70$ (Figure 1D).

The Identification and Reactivity Studies of Intermediates Formed in the System $1/\text{H}_2\text{O}_2$. The expanded EPR spectrum

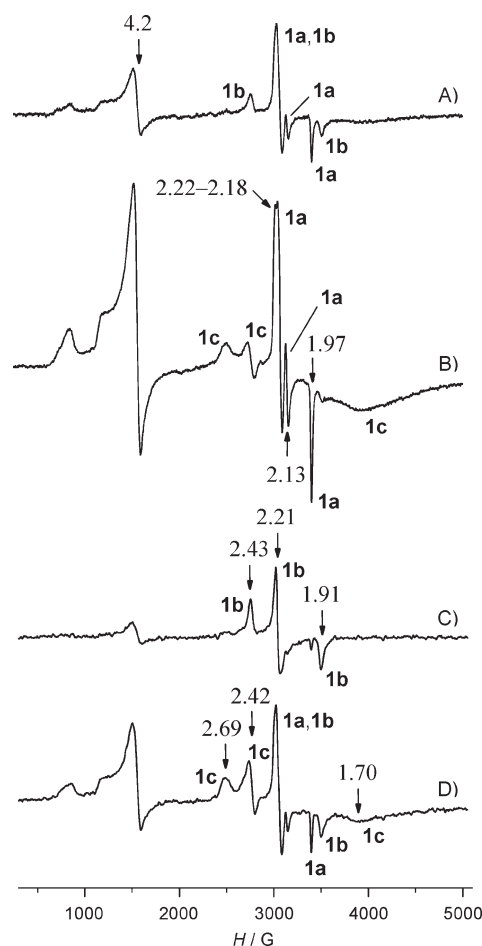


Figure 1. EPR spectra ($-196\text{ }^\circ\text{C}$) of the sample $1/\text{H}_2\text{O}_2$ ($[\text{H}_2\text{O}_2]/[\mathbf{1}] = 2$, $[\mathbf{1}] = 0.027\text{ M}$) frozen 30 s after mixing the reagents at $-60\text{ }^\circ\text{C}$ (A) and 5 min after storing the sample in “A” at $-70\text{ }^\circ\text{C}$ (B). EPR spectra ($-196\text{ }^\circ\text{C}$) of the sample $1/\text{H}_2\text{O}_2$ ($[\text{H}_2\text{O}_2]/[\mathbf{1}] = 10$, $[\mathbf{1}] = 0.027\text{ M}$) frozen 30 s after mixing the reagents at $-60\text{ }^\circ\text{C}$ (C) and 5 min after storing the sample in “C” at $-70\text{ }^\circ\text{C}$ (D). A 1:1.7 $\text{CH}_3\text{CN}/\text{CH}_2\text{Cl}_2$ mixture was used as a solvent.

denoted in Figure 1 as **1a** is presented in Figure 2A. This spectrum is a superposition of the spectra of two species: $g_1 = 2.218$, $g_2 = 2.175$, and $g_3 = 1.966$ (**1a-CH₃CN**) and $g_1 = 2.197$, $g_2 = 2.128$, and $g_3 = 1.970$ (**1a-H₂O**; Figure 2C,D and Table 1).³² The simulated spectrum (Figure 2B) is in excellent agreement with the experimental one (Figure 2A).

Very similar spectra were observed in the system $2/\text{H}_2\text{O}_2$ and were assigned to the hydroperoxo complexes $[(\text{TPA})\text{Fe}^{\text{III}}(\text{OOH})(\text{CH}_3\text{CN})]^{2+}$ (**2a-CH₃CN**) and $[(\text{TPA})\text{Fe}^{\text{III}}(\text{OOH})(\text{H}_2\text{O})]^{2+}$ (**2a-H₂O**) (Table 1).³¹ By analogy with the TPA-based system, **1a-CH₃CN** and **1a-H₂O** can be attributed to the hydroperoxo complexes $[(\text{BPMEN})\text{Fe}^{\text{III}}(\text{OOH})(\text{CH}_3\text{CN})]^{2+}$ and $[(\text{BPMEN})\text{Fe}^{\text{III}}(\text{OOH})(\text{H}_2\text{O})]^{2+}$, respectively.³² **2a-CH₃CN** was formulated by Que and co-workers to be $[(\text{L})\text{Fe}^{\text{III}}-\text{OOH}]^{2+}$ species based on ESI-MS data.^{11,29} Very recently, ESI-MS data of Rybak-Akimova and Makhlynets have confirmed our assignment of **1a-CH₃CN** and **1a-H₂O** to the low-spin hydroperoxo ferric species.²⁷

The rate of the self-decay of complexes **1a-CH₃CN** and **1a-H₂O** at $-60\text{ }^\circ\text{C}$ does not essentially change in the presence of cyclohexene.³² Similar results were obtained for hydroperoxo

Table 1. EPR Spectroscopic Data for $S = 1/2$ Iron–Oxygen Species Formed in the Systems Studied Herein in Comparison with Those for Related Complexes^a

| complex | g_1 | g_2 | g_3 | ref |
|--|-------|-------|-------|------------|
| $[(\text{BPMEN})\text{Fe}^{\text{III}}(\text{OOH})(\text{CH}_3\text{CN})]^{2+}$ (1a-CH₃CN) | 2.218 | 2.175 | 1.966 | 32 |
| $[(\text{BPMEN})\text{Fe}^{\text{III}}(\text{OOH})(\text{H}_2\text{O})]^{2+}$ (1a-H₂O) | 2.197 | 2.128 | 1.970 | 32 |
| $[(\text{BPMEN})\text{Fe}^{\text{III}}(\text{OO}^t\text{Bu})(\text{CH}_3\text{CN})]^{2+}$ (1g-CH₃CN) | 2.156 | 2.111 | 1.966 | this work |
| $[(\text{BPMEN})\text{Fe}^{\text{III}}(\text{OO}^t\text{Bu})(\text{H}_2\text{O})]^{2+}$ (1g-H₂O) | 2.177 | 2.111 | 1.966 | this work |
| $[(\text{BPMEN})\text{Fe}^{\text{III}}(\text{OH})(\text{S})]^{2+}$ (1b) ^b | 2.43 | 2.21 | 1.91 | 32 |
| $[(\text{BPMEN})\text{Fe}^{\text{III}}(\text{O}^t\text{Bu})(\text{S})]^{2+}$ (1h) ^b | 2.38 | 2.17 | 1.91 | this work |
| $[(\text{BPMEN})\text{Fe}^{\text{III}}(\text{OAc})(\text{S})]^{2+}$ (1e) ^b | 2.37 | 2.16 | 1.92 | this work |
| 1c | 2.69 | 2.42 | 1.70 | 36 |
| $[(\text{TPA})\text{Fe}^{\text{III}}(\text{OOH})(\text{CH}_3\text{CN})]^{2+}$ (2a-CH₃CN) | 2.194 | 2.152 | 1.970 | 29, 31 |
| $[(\text{TPA})\text{Fe}^{\text{III}}(\text{OOH})(\text{H}_2\text{O})]^{2+}$ (2a-H₂O) | 2.19 | 2.12 | 1.97 | 31 |
| $[(\text{TPA})\text{Fe}^{\text{III}}(\text{OO}^t\text{Bu})(\text{CH}_3\text{CN})]^{2+}$ (2g-CH₃CN) | 2.156 | 2.115 | 1.966 | 31 |
| $[(\text{TPA})\text{Fe}^{\text{III}}(\text{OO}^t\text{Bu})(\text{H}_2\text{O})]^{2+}$ (2g-H₂O) | 2.198 | 2.130 | 1.969 | 50, 51, 31 |
| 2c | 2.71 | 2.42 | 1.53 | 36 |
| 2f | 2.206 | 2.159 | 1.946 | this work |
| 2i | 2.07 | 2.00 | 2.00 | this work |
| $[(\text{TAML})\text{Fe}^{\text{V}}=\text{O}]^-$ | 1.99 | 1.97 | 1.74 | 35 |
| $[(\text{N4Py})\text{Fe}^{\text{III}}(\text{OH})]^{2+}$ | 2.41 | 2.15 | 1.92 | 40 |
| $[(\text{BLM})\text{Fe}^{\text{III}}(\text{OH})]$ | 2.43 | 2.19 | 1.89 | 41, 42 |
| $[(\text{TPEN})\text{Fe}^{\text{III}}(\text{OH})]^{2+}$ | 2.39 | 2.19 | 1.91 | 39 |
| $[(\text{TPEN})\text{Fe}^{\text{III}}(\text{OMe})]^{2+}$ | 2.34 | 2.14 | 1.93 | 39 |
| $[(\text{BZTPEN})\text{Fe}^{\text{III}}(\text{OH})]^{2+}$ | 2.39 | 2.19 | 1.91 | 39 |
| $[(\text{BZTPEN})\text{Fe}^{\text{III}}(\text{OMe})]^{2+}$ | 2.33 | 2.14 | 1.93 | 39 |
| $[\text{Fe}^{\text{III}}(\text{phen})_3]^{3+}$ | 2.69 | 2.69 | 1.51 | 1 |
| $[\text{Fe}^{\text{III}}(\text{bpy})_2(\text{CN})_2]^+$ | 2.63 | 2.63 | 1.42 | 1 |
| $[\text{Fe}^{\text{III}}(\text{TPP})(\text{ImH})_2]^+$ | 2.92 | 2.30 | 1.56 | 1 |
| $[\text{Fe}^{\text{III}}(\text{TPP})(\text{Im})_2]^-$ | 2.73 | 2.28 | 1.76 | 1 |

^aEPR spectra were recorded at -196°C or lower. TAML = macrocyclic tetraamide ligand, N4Py = *N,N*-bis(2-pyridylmethyl)-*N*-(bis-2-pyridylmethyl)amine, BLM = bleomycin, Phen = 1,10-phenanthroline, bpy = 2,2'-bipyridine, H₂TPP = tetraphenylporphyrin, ImH = imidazole.

^bS = CH₃CN or H₂O.

and alkylperoxo complexes formed in the systems **2**/H₂O₂ and **2**/^{*t*}BuOOH.³¹ On the basis of these data, it was proposed that hydroperoxo and alkylperoxo complexes $[(\text{BPMEN})\text{Fe}^{\text{III}}(\text{OOH})(\text{S})]^{2+}$, $[(\text{TPA})\text{Fe}^{\text{III}}(\text{OOH})(\text{S})]^{2+}$, and $[(\text{TPA})\text{Fe}^{\text{III}}(\text{OO}^t\text{Bu})(\text{S})]^{2+}$, where S = CH₃CN or H₂O, can hardly be directly involved in the reaction with organic substrates.^{31,32} Later, the assumption that the low-spin ferric alkylperoxo and hydroperoxo complexes are sluggish oxidants was confirmed by Nam and co-workers using a broader set of iron complexes and organic substrates.^{34,38}

The EPR spectrum of **1b** ($g_1 = 2.43$, $g_2 = 2.21$, $g_3 = 1.91$) is close to the EPR spectrum of the low-spin ferric hydroxo complexes $[(\text{TPEN})\text{Fe}^{\text{III}}(\text{OH})]^{2+}$ and $[(\text{BZTPEN})\text{Fe}^{\text{III}}(\text{OH})]^{2+}$ ($g_1 = 2.39$, $g_2 = 2.19$, $g_3 = 1.91$, Table 1).³⁹ TPEN and BZTPEN ligands are related to BPMEN (Chart 2). EPR spectra previously assigned to $[(\text{N4Py})\text{Fe}^{\text{III}}(\text{OH})]^{2+}$ and $[(\text{BLM})\text{Fe}^{\text{III}}(\text{OH})]$ are also similar to that of **1b** (Table 1).^{40–42} Therefore, it is reasonable to assume that **1b** is the hydroxo complex $[(\text{BPMEN})\text{Fe}^{\text{III}}(\text{OH})(\text{S})]^{2+}$, where S = H₂O or CH₃CN.

Complex **1c** ($g_1 = 2.69$, $g_2 = 2.42$, $g_3 = 1.70$) is the most interesting species among the intermediates found, since its decay rate at -70°C increases by an order of magnitude in the presence of 12 equiv of cyclohexene, whereas the lifetimes of **1a** and **1b** do not change under the same conditions.³⁶ The structure of **1c** will be discussed below.

As was mentioned above, the EPR spectra of the catalyst system **1**/H₂O₂ display resonance at $g = 4.2$ from unidentified high-spin $S = 5/2$ ferric species. The previous studies of Que et al. have shown that the low-spin $S = 1/2$ ferric hydroperoxo complexes, rather than high-spin $S = 5/2$ counterparts, are the most likely precursors of the active species of epoxidation.^{11,43,44} Therefore, in this work, only low-spin $S = 1/2$ iron species have been studied.

The Systems 1/CH₃CO₃H, 1/*m*-CPBA, and 1/PhIO. The EPR spectrum of the sample **1**:**2** **1**/CH₃CO₃H ($[\text{1}] = 0.04\text{ M}$), frozen after mixing the reagents for 30 s at -60°C and 1 min of storing at -70°C , displays resonances of **1c** (Figure 3A). Further storing the sample in Figure 3A at -70°C results in the appearance of resonances of complex **1b** and a new complex **1e** (Figure 3B,C). The g values of **1e** are within the range typical for $[(\text{L})\text{Fe}^{\text{III}}(\text{OH})]^{2+}$ and $[(\text{L})\text{Fe}^{\text{III}}(\text{OMe})]^{2+}$ (L = TPEN or BZTPEN, Table 1).³⁹ The values of g_1 and g_2 decrease while that of g_3 increases when going from $[(\text{TPEN})\text{Fe}^{\text{III}}(\text{OH})]^{2+}$ and $[(\text{BZTPEN})\text{Fe}^{\text{III}}(\text{OH})]^{2+}$ to $[(\text{TPEN})\text{Fe}^{\text{III}}(\text{OMe})]^{2+}$ and $[(\text{BZTPEN})\text{Fe}^{\text{III}}(\text{OMe})]^{2+}$. The same tendency is observed when going from **1b** to **1e** (Table 1). Thus, we assign **1e** to the low-spin ferric complex $[(\text{BPMEN})\text{Fe}^{\text{III}}(\text{OAc})(\text{S})]^{2+}$.

The EPR spectra of the sample **1**/*m*-CPBA = **1**:**2** (Figure 4) are similar to those of the sample **1**/CH₃CO₃H = **1**:**2**, but only **1c** and **1b** are observed (compare Figures 3 and 4). The maximum

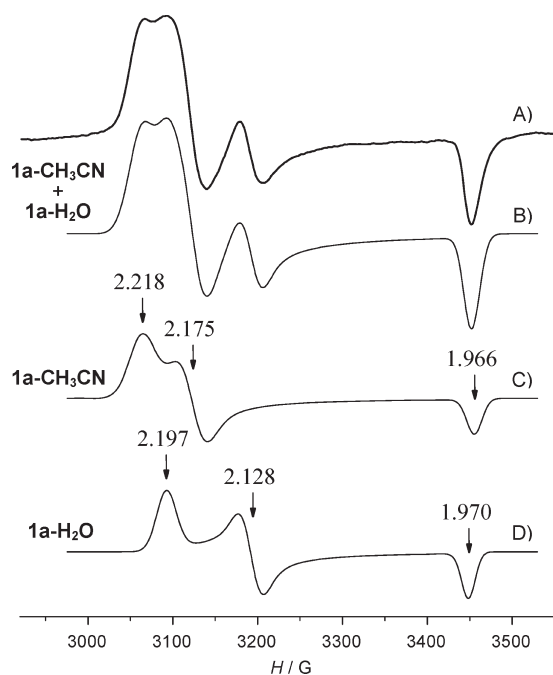
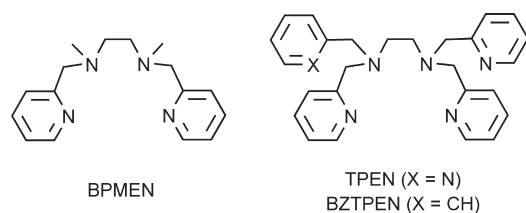


Figure 2. Expanded EPR spectrum of **1a** (A). Simulated superposition of spectra of **1a-CH₃CN** and **1a-H₂O** ($[\mathbf{1a-CH_3CN}]/[\mathbf{1a-H_2O}] = 1.85$) (B). Simulated spectrum of **1a-CH₃CN** ($g_1 = 2.218$, $g_2 = 2.175$, and $g_3 = 1.966$; individual line widths $\Delta H_1 = 15$ G, $\Delta H_2 = 14$ G, and $\Delta H_3 = 9$ G; Gaussian line shape) (C). Simulated spectrum of **1a-H₂O** ($g_1 = 2.197$, $g_2 = 2.128$, and $g_3 = 1.970$; individual line widths $\Delta H_1 = 11.5$ G, $\Delta H_2 = 11.5$ G, and $\Delta H_3 = 8$ G; Gaussian line shape) (D).

Chart 2. Aminopyridine Ligands



concentration of **1c** observed in the systems based on complex **1** and peracids approaches 8% of the total iron concentration. As was noted above, **1c** rapidly reacts with cyclohexene even at -70 °C. The main cyclohexene oxidation product formed in the samples 1:10:30 **1**/CH₃CO₃H/C₆H₁₀ and 1:2:40 **1**/*m*-CPBA/C₆H₁₀ after 1 h of storage at -70 °C is cyclohexene oxide (Table 2, entries 3 and 5). Thus, the reaction of **1c** with cyclohexene leads to the formation of cyclohexene oxide. Cyclohexene is not oxidized by CH₃CO₃H, *m*-CPBA, and H₂O₂ at -70 °C in the absence of the iron complex over at least several hours.

It is interesting to compare the reactivity and selectivity of **1c** and those of the oxoiron(IV) intermediate $[(\text{BPMEN})\text{Fe}^{\text{IV}}=\text{O}(\text{CH}_3\text{CN})]^{2+}$ (**1d**) toward the oxidation of cyclohexene. As was reported previously, **1d** can be readily trapped in the systems **1**/CH₃CO₃H and **1**/PhIO by ¹H NMR spectroscopy.³³ The ¹H NMR spectra (-70 °C, -50 °C) of the sample 1:2 **1**/CH₃CO₃H recorded 5 min after mixing the reagents at -40 °C in a 1.7:1 CD₂Cl₂/CD₃CN mixture display high-field paramagnetically shifted resonances that are typical for the low-spin ($S = 1$)

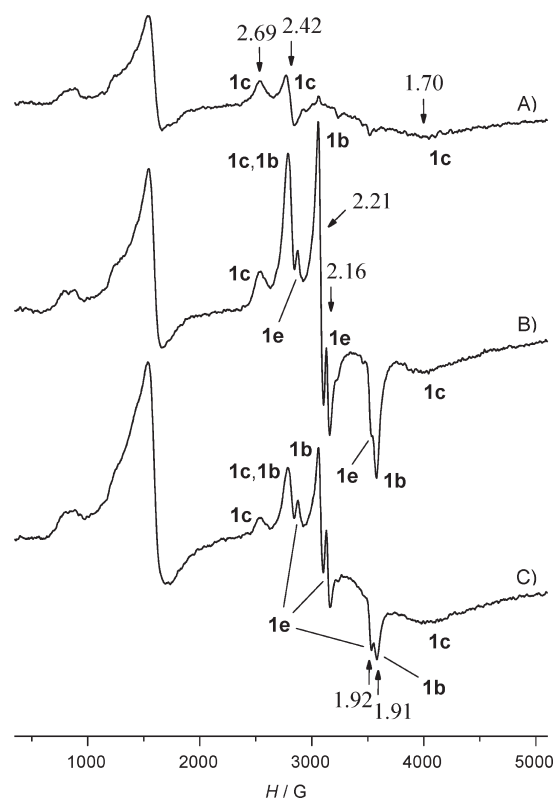


Figure 3. EPR spectra (-196 °C) of the sample **1**/CH₃CO₃H ($[\text{CH}_3\text{CO}_3\text{H}]/[\mathbf{1}] = 2$, $[\mathbf{1}] = 0.04$ M) frozen after mixing the reagents for 30 s at -60 °C in a 1.7:1 CH₂Cl₂/CH₃CN mixture and storing it at -70 °C for 1 min (A), 5 min (B), and 22 min (C).

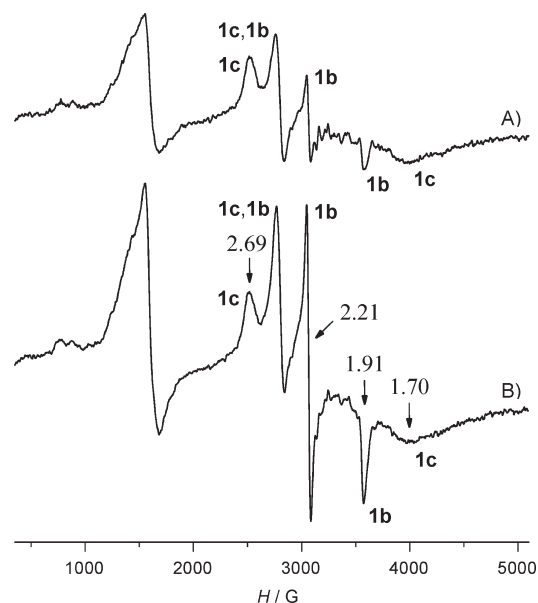


Figure 4. EPR spectra (-196 °C) of the sample **1**/*m*-CPBA ($[\text{m-CPBA}]/[\mathbf{1}] = 2$, $[\mathbf{1}] = 0.04$ M) frozen after mixing the reagents for 30 s at -60 °C in a 1.7:1 CH₂Cl₂/CH₃CN mixture and storing it at -70 °C for 6 min (A) and 21 min (B).

oxoiron(IV) species (Figure 5B,C).^{33,45} A similar spectrum was observed upon interaction of **1** with PhIO (Figure 5D). On the basis of these data, it was suggested that the observed spectrum

Table 2. Catalytic Oxidation of Cyclohexene at $-70\text{ }^{\circ}\text{C}^a$

| entry | cat. | oxidant | [Fe]/[oxidant]/[cyclohexene] | epoxide ^b | enone ^b | enol ^b | epoxide selectivity [%] |
|-------|------|-----------------------------------|------------------------------|----------------------|--------------------|-------------------|-------------------------|
| 1 | 1 | H ₂ O ₂ | 1:10:30 | 2.8 | 0.9 | 1.1 | 58 |
| 2 | 2 | H ₂ O ₂ | 1:10:30 | 0.7 | 2.0 | 2.2 | 14 |
| 3 | 1 | CH ₃ CO ₃ H | 1:10:30 | 77 | 2 | 1 | 96 |
| 4 | 2 | CH ₃ CO ₃ H | 1:10:30 | 62 | 3 | 1 | 94 |
| 5 | 1 | <i>m</i> -CPBA | 1:2:40 | 34 | 4 | 3 | 83 |
| 6 | 2 | <i>m</i> -CPBA | 1:2:40 | 42 | 2 | 3 | 89 |

^a Stirring for 1 h at $-70\text{ }^{\circ}\text{C}$ in a 1.3:1 CH₂Cl₂/CH₃CN mixture. An excess of precooled triphenylphosphine was added to consume oxidant residues before subjecting the solution to GC analysis. [Fe] = 0.027 M in experiments with H₂O₂(CH₃CO₃H) and 0.02 M in experiments with *m*-CPBA.

^b Product yield (%) based on the oxidant. Epoxide denotes cyclohexene oxide; enone, 2-cyclohexen-1-one; and enol, 2-cyclohexen-1-ol.

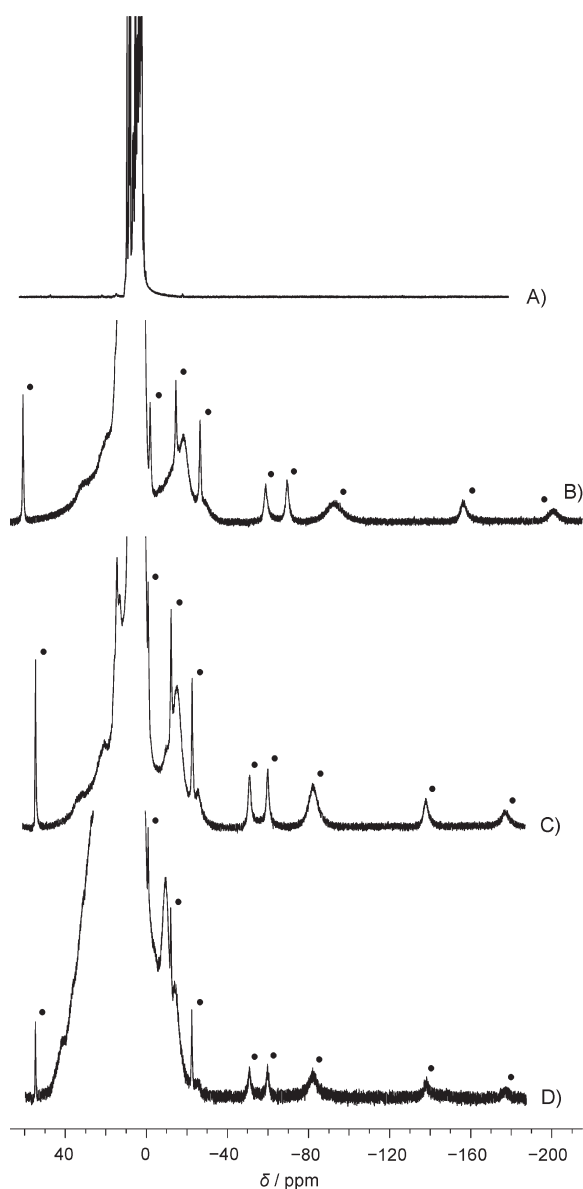


Figure 5. ¹H NMR spectrum ($-50\text{ }^{\circ}\text{C}$) of complex **1** (A). ¹H NMR spectra of sample **1**/CH₃CO₃H ([CH₃CO₃H]/[**1**] = 2, [**1**] = 0.05 M) recorded at $-70\text{ }^{\circ}\text{C}$ (B) and at $-50\text{ }^{\circ}\text{C}$ (C) 5 min after mixing the reagents at $-40\text{ }^{\circ}\text{C}$ in a 1.7:1 CD₂Cl₂/CD₃CN mixture. ¹H NMR spectrum ($-50\text{ }^{\circ}\text{C}$) of the sample **1**:2 **1**/PhIO ([**1**] = 0.05 M) 3 min after mixing the reagents at $0\text{ }^{\circ}\text{C}$ in a 1.7:1 CD₂Cl₂/CD₃CN mixture (D). Points denote peaks of **1d**.

belongs to the oxoiron(IV) complex [(BPMEN)Fe^{IV}=O(CH₃CN)]²⁺ (**1d**).³³ The number of ¹H NMR peaks of **1d** corresponds to the number of chemically nonequivalent protons of the coordinated BPMEN ligand: N-CHH-CHH-N, N-CHH-CHH-N, Py-CHH, Py-CHH, CH₃, Py-(α -H), Py-(β -H), Py-(β' -H), and Py-(γ -H) (Chart 1; Table S1, Supporting Information).^{46,47}

Complex **1d** is stable in a 1.7:1 CD₂Cl₂/CD₃CN mixture at $-50\text{ }^{\circ}\text{C}$ and decays at higher temperatures (the half-life time $\tau_{1/2} \approx 5$ min at $0\text{ }^{\circ}\text{C}$ in the system **1**/PhIO). The intensities of the ¹H NMR peaks of **1d** correspond to the conversion of up to 30% of **1** into **1d** in the system 1:2 **1**/CH₃CO₃H and up to 10% in the system 1:2 **1**/PhIO. After the addition of 12 equiv of cyclohexene to the solution containing **1d** at $-50\text{ }^{\circ}\text{C}$, the latter disappears within several minutes. Thus, **1d** and **1c** both react with cyclohexene at $-50\text{ }^{\circ}\text{C}$. However, at $-70\text{ }^{\circ}\text{C}$, **1c** is much more reactive than **1d**: the intensities of the ¹H NMR peaks of **1d** decreased 2-fold after 1 h of storing the sample containing **1d** and 12 equiv of cyclohexene, whereas the EPR peaks of **1c** completely disappear after 10 min under the same conditions.

In order to compare the selectivities of **1c** and **1d** toward cyclohexene epoxidation, we have compared the yields of cyclohexene oxidation products formed in the catalyst systems **1**/H₂O₂/C₆H₁₀ and **1**/PhIO/C₆H₁₀. The system **1**/H₂O₂ displays EPR peaks of **1c** (Figure 1), whereas the ¹H NMR resonances of **1d** were not found. On the contrary, the system **1**/PhIO shows the ¹H NMR resonances of **1d** (Figure 5D), whereas EPR peaks of **1c** were not detected. It was found that in the sample 1:10:300 **1**/H₂O₂/C₆H₁₀, cyclohexene oxide is the major product (Table 3, entry 1), whereas in the sample 1:10:300 **1**/PhIO/C₆H₁₀, mainly the allylic oxidation products (i.e., 2-cyclohexen-1-one and 2-cyclohexen-1-ol) were observed (Table 3, entries 10 and 11). Hence, **1c** is able to selectively epoxidize cyclohexene, whereas **1d** mainly drives its allylic oxidation.

In our previous paper,³³ we erroneously concluded that oxoiron(IV) complex **1d** is the active species of epoxidation of the catalyst system **1**/CH₃CO₃H. This conclusion was made on the basis of the dramatic increase of the decay rate of **1d** in the presence of cyclohexene at $-50\text{ }^{\circ}\text{C}$. However, the present studies revealed that the system **1**/PhIO exhibiting the ¹H NMR resonances of **1d** and no EPR resonances of the putative oxoiron(V) complex **1c** drives the allylic oxidation of cyclohexene, whereas the system **1**/H₂O₂ exhibiting resonances of **1c** and no resonances of **1d** affords predominantly cyclohexene oxide. Therefore, **1d** can be responsible only for the side products formed in the sample **1**/CH₃CO₃H/C₆H₁₀. The high reactivity of **1c** toward oxidation of cyclohexene even at $-70\text{ }^{\circ}\text{C}$ and the

Table 3. Catalytic Oxidation of Cyclohexene at 25 °C^a

| entry | catalyst | conditions | oxidant | equiv CH ₃ COOH | epoxide ^b | enone ^b | enol ^b | cis-diol ^b | selectivity [%] ^c |
|-------|----------|------------|-----------------------------------|----------------------------|----------------------|--------------------|-------------------|-----------------------|------------------------------|
| 1 | 1 | air | H ₂ O ₂ | | 79 | 30 | 35 | 4 | 56 |
| 2 | 1 | air | H ₂ O ₂ | 100 | 87 | 10 | 11 | 4 | 81 |
| 3 | 1 | Ar | CH ₃ CO ₃ H | | 81 | 4 | 7 | <1 | 88 |
| 4 | 1 | air | ^t BuOOH | | 48 | 104 | 77 | | 21 |
| 5 | 1 | air | ^t BuOOH | 10 | 84 | 49 | 58 | | 44 |
| 6 | 1 | air | ^t BuOOH | 100 | 79 | 46 | 52 | | 45 |
| 7 | 1 | Ar | ^t BuOOH | | 8 | 18 | 49 | | 11 |
| 8 | 1 | Ar | ^t BuOOH | 10 | 68 | 8 | 15 | | 75 |
| 9 | 1 | Ar | ^t BuOOH | 100 | 57 | 6 | 16 | | 72 |
| 10 | 1 | air | PhIO | | 16 | 31 | 36 | | 19 |
| 11 | 1 | Ar | PhIO | | 13 | 23 | 37 | | 18 |
| 12 | 2 | air | H ₂ O ₂ | | 23 | 75 | 70 | 8 | 18 |
| 13 | 2 | air | H ₂ O ₂ | 100 | 40 | 12 | 17 | 6 | 61 |
| 14 | 2 | Ar | CH ₃ CO ₃ H | | 51 | 8 | 13 | 4 | 72 |
| 15 | 2 | air | ^t BuOOH | | 8 | 172 | 181 | | 2 |
| 16 | 2 | air | ^t BuOOH | 10 | 18 | 159 | 143 | | 6 |
| 17 | 2 | air | ^t BuOOH | 100 | 24 | 156 | 108 | | 8 |
| 18 | 2 | Ar | ^t BuOOH | | | 14 | 65 | | 0 |
| 19 | 2 | Ar | ^t BuOOH | 10 | | 19 | 58 | | 0 |
| 20 | 2 | Ar | ^t BuOOH | 100 | 2 | 7 | 62 | | 3 |
| 21 | 2 | air | PhIO | | 15 | 63 | 69 | | 10 |
| 22 | 2 | Ar | PhIO | | 4 | 29 | 43 | | 5 |

^a Fe/oxidant/cyclohexene = 1:10:300, [Fe] = 2.7×10^{-3} M. The oxidant (except PhIO) was delivered by syringe pump over 25 min, and 5 extra minutes of stirring were allowed before subjecting the solution to GC analysis. PhIO was added all at once, and products were analyzed by GC after 30 min of stirring. ^b Product yield (%) expressed in moles of product per mole of oxidant. Epoxide denotes cyclohexene oxide; enone, 2-cyclohexen-1-one; enol, 2-cyclohexen-1-ol; cis-diol, cis-1,2-cyclohexanediol. ^c Selectivity toward epoxidation and cis-dihydroxylation.

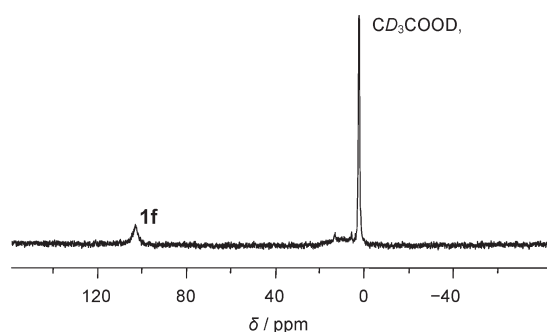


Figure 6. ²H NMR spectrum (−50 °C) of the system 1/CD₃CO₃H recorded 10 min after mixing the reagents at −50 °C in a 1:1 CH₂Cl₂/CH₃CN mixture ([1] = 0.05 M, [CD₃CO₃H]/[1] = 1.5).

formation of predominantly cyclohexene oxide in the system 1/H₂O₂/C₆H₁₀ at this temperature are consistent with the assumption that 1c is the active species of epoxidation.

In the early work of Que et al.,³⁰ formation of [(TPA)-Fe^{IV}=O]²⁺ was detected upon the reaction of complex 2 and CH₃CO₃H at −40 °C. In a subsequent work of the same group, it was found that [(TPA)Fe^{IV}=O]²⁺ is relatively inert, and another more reactive species should exist in the catalyst system 2/*m*-CPBA capable of aromatic ring hydroxylation.⁴⁸ It was proposed that this species is (TPA)Fe^V=O, which is derived from O–O bond heterolysis of the acylperoxo complex [(TPA)-Fe^{III}(*m*-Cl–C₆H₄–C(O)OO)]²⁺. However, [(TPA)Fe^{III}(*m*-Cl–C₆H₄–C(O)OO)]²⁺ and (TPA)Fe^V=O were not detected.⁴⁸

Thus, we have undertaken the search for acylperoxo complex [(BPMEN)Fe^{III}(O₃CCH₃)]²⁺ using ²H NMR spectroscopy and ²H-labeled peracetic acid (CD₃CO₃H).³³ The ²H NMR spectrum (−50 °C) recorded 10 min after the addition of 1.5 equiv of CD₃CO₃H to 1 in a 1:1 CH₂Cl₂/CH₃CN mixture at −50 °C exhibits a broad peak at δ = 102.7 ppm (Δν_{1/2} = 230 Hz) of a new complex 1f (Figure 6). This peak disappears upon warming (τ_{1/2} = 10 min at −30 °C). For high-spin complex (TPP)Fe^{III}–O–O–CD₂–CD₃ (TPP = dianion of tetra-*p*-tolylporphyrin), the CD₂ peak was observed at δ = 180 ppm and the CD₃ peak at δ = 4 ppm.⁴⁹ On the basis of these data, the resonance at δ = 102.7 ppm can be assigned to the OOCDD₃ or O₃CCD₃ moiety bound to the high-spin iron(III). Unfortunately, we cannot reliably distinguish between these two possibilities, and 1f can be assigned to the high-spin ferric complex [(BPMEN)Fe^{III}(O₃CCD₃)]²⁺ or [(BPMEN)Fe^{III}(OOCDD₃)]²⁺. The possible route of [(BPMEN)-Fe^{III}(O₃CCH₃)]²⁺ formation is the O–O bond homolysis of CH₃CO₃H in the presence of 1 to afford [(BPMEN)Fe^{III}(OH)]²⁺ and successive replacement of HO[−] with CH₃C(O)OO[−].

The Systems 1/^tBuOOH and 1/^tBuOOH/CH₃COOH. The EPR spectrum of the sample 1:2.5 1/^tBuOOH recorded 1 min after mixing the reagents at −50 °C in a 1.7:1 CH₂Cl₂/CH₃CN mixture is a superposition of two rhombic EPR spectra with *g*₁ = 2.156, *g*₂ = 2.111, and *g*₃ = 1.966 and *g*₁ = 2.177, *g*₂ = 2.111, and *g*₃ = 1.966 (Figure 7A). The simulated spectrum (Figure 7B) is in good agreement with the experimental one. The observed two rhombic spectra are very similar to those of the alkylperoxo complexes [(TPA)Fe^{III}(OO^{*t*}Bu)(CH₃CN)]²⁺ and [(TPA)Fe^{III}(OO^{*t*}Bu)(H₂O)]²⁺, respectively (Table 1).^{31,50,51} Therefore, the EPR spectrum

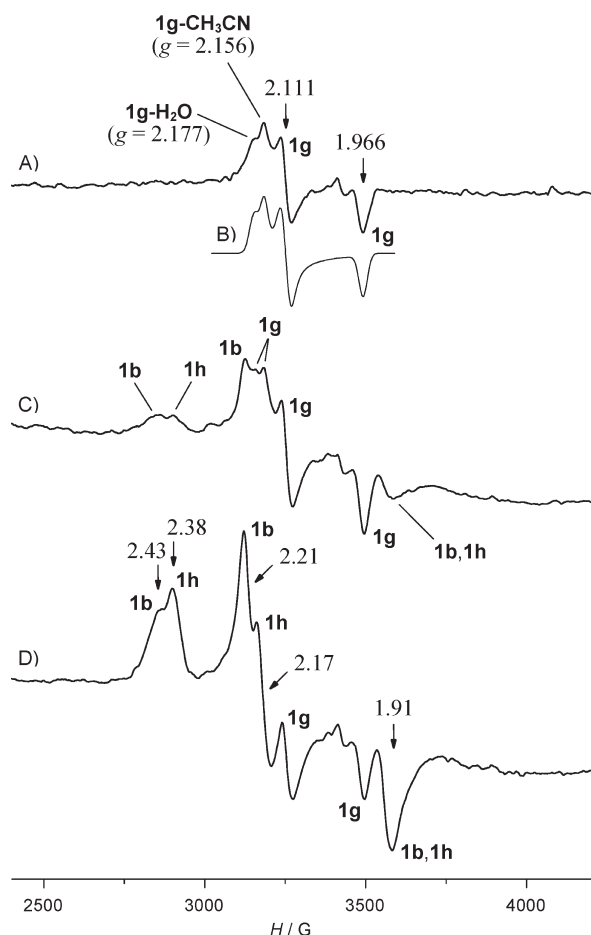


Figure 7. EPR spectra ($-196\text{ }^{\circ}\text{C}$) of the sample $1/t\text{BuOOH}$ ($[1]/[t\text{BuOOH}] = 1:2.5$, $[1] = 0.045\text{ M}$) frozen 1 min (A), 7 min (C), and 13 min (D) after mixing the reagents at $-50\text{ }^{\circ}\text{C}$ in a 1.7:1 $\text{CH}_2\text{Cl}_2/\text{CH}_3\text{CN}$ mixture. Simulated superposition of spectra of $1g\text{-CH}_3\text{CN}$ ($g_1 = 2.156$, $g_2 = 2.111$, $g_3 = 1.966$; individual line widths $\Delta H_1 = 11.5\text{ G}$, $\Delta H_2 = 11\text{ G}$, $\Delta H_3 = 13\text{ G}$; Gaussian line shape) and $1g\text{-H}_2\text{O}$ ($g_1 = 2.177$, $g_2 = 2.111$, $g_3 = 1.966$; individual line widths $\Delta H_1 = 14.5\text{ G}$, $\Delta H_2 = 13\text{ G}$, $\Delta H_3 = 13\text{ G}$; Gaussian line shape); $[1a\text{-H}_2\text{O}]/[1a\text{-CH}_3\text{CN}] = 1.36$ (B).

with $g_1 = 2.156$, $g_2 = 2.111$, and $g_3 = 1.966$ was assigned to $[(\text{BPMEN})\text{Fe}^{\text{III}}(\text{OO}^t\text{Bu})(\text{CH}_3\text{CN})]^{2+}$ ($1g\text{-CH}_3\text{CN}$) and the EPR spectrum with $g_1 = 2.177$, $g_2 = 2.111$, and $g_3 = 1.966$ to $[(\text{BPMEN})\text{Fe}^{\text{III}}(\text{OO}^t\text{Bu})(\text{H}_2\text{O})]^{2+}$ ($1g\text{-H}_2\text{O}$). Storing the sample in Figure 7A at $-50\text{ }^{\circ}\text{C}$ leads to the rise of EPR peaks of $1b$ ($g_1 = 2.43$, $g_2 = 2.21$, $g_3 = 1.91$) and a new complex $1h$ ($g_1 = 2.38$, $g_2 = 2.17$, $g_3 = 1.91$; Figure 7C,D). The g values of $1h$ are very close to those of complexes $[(\text{BPMEN})\text{Fe}^{\text{III}}(\text{OH})(\text{S})]^{2+}$ ($1b$) and $[(\text{BPMEN})\text{Fe}^{\text{III}}(\text{OAc})(\text{S})]^{2+}$ ($1e$; Table 1). On the basis of this fact, $1h$ was assigned to the alkoxo complex $[(\text{BPMEN})\text{Fe}^{\text{III}}(\text{O}^t\text{Bu})(\text{S})]^{2+}$. Hence, the reaction of 1 with $t\text{BuOOH}$ at $-50\text{ }^{\circ}\text{C}$ results in the formation of the alkylperoxo complexes $1g\text{-CH}_3\text{CN}$ and $1g\text{-H}_2\text{O}$ and complexes of the type $[(\text{BPMEN})\text{Fe}^{\text{III}}(\text{OR})(\text{S})]^{2+}$, where $\text{R} = \text{H}$ or $t\text{Bu}$ and $\text{S} = \text{H}_2\text{O}$ or CH_3CN .

The addition of acetic acid to the above sample dramatically changes the nature of the intermediates present in the reaction solution. Besides the resonances of $1g$, the EPR spectra of the sample 1:2.5:10 $1/t\text{BuOOH}/\text{CH}_3\text{COOH}$ display resonances of $1c$ (Figure 8). Thus, acetic acid promotes the formation of $1c$.

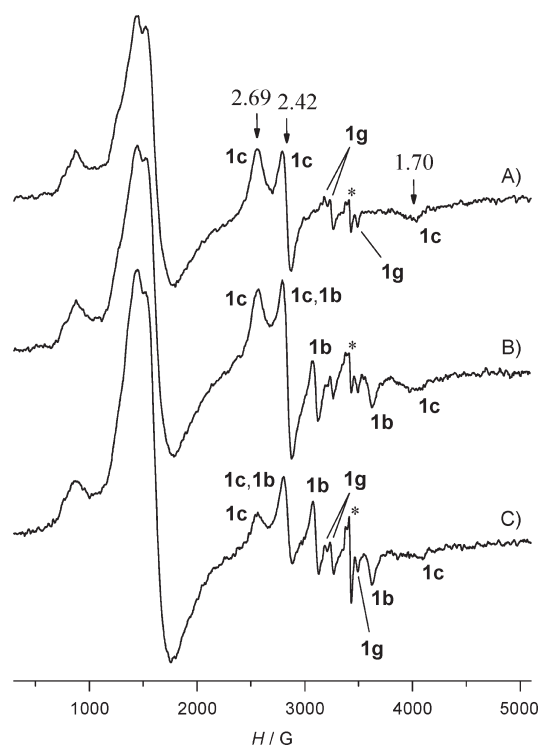


Figure 8. EPR spectra ($-196\text{ }^{\circ}\text{C}$) of the sample $1/t\text{BuOOH}/\text{CH}_3\text{COOH}$ ($[1]/[t\text{BuOOH}]/[\text{CH}_3\text{COOH}] = 1:2.5:10$, $[1] = 0.045\text{ M}$) frozen 1 min after mixing the reagents at $-60\text{ }^{\circ}\text{C}$ in a 1.7:1 $\text{CH}_2\text{Cl}_2/\text{CH}_3\text{CN}$ mixture (A) and 2 min (B) and 7 min (C) after storing the sample in "A" at $-70\text{ }^{\circ}\text{C}$. Signals denoted by an asterisk belong to still unidentified minor species.

It is natural to expect that the systems $1/t\text{BuOOH}$ and $1/t\text{BuOOH}/\text{CH}_3\text{COOH}$ should exhibit different selectivities toward the epoxidation of cyclohexene. The latter system should be more selective due to a much higher concentration of the active epoxidizing agent $1c$. In agreement with this prediction, the yield of cyclohexene oxide in the sample 1:10:300 $1/t\text{BuOOH}/\text{C}_6\text{H}_{10}$ was lower than in the sample 1:10:10:300 $1/t\text{BuOOH}/\text{CH}_3\text{COOH}/\text{C}_6\text{H}_{10}$: compare 48% and 84% in the air (Table 3, entries 4 and 5) and 8% and 68% in argon (Table 3, entries 7 and 8). The sharper difference in cyclohexene oxide yield is observed for the reaction in argon. The reason for the less pronounced difference in the air is still unclear.

The catalyst system $1/t\text{BuOOH}/\text{CH}_3\text{COOH}$ is a rare example of the nonheme iron-based system capable of selective olefin epoxidation with $t\text{BuOOH}$ as an oxidant. Typically, the catalyst systems based on nonheme iron complexes and $t\text{BuOOH}$ drive the free radical oxidation.⁵² The positive effect of acetic acid on the epoxidation selectivity of the $1/\text{H}_2\text{O}_2$ system was reported previously.^{10,28} It was suggested that CH_3COOH promotes the heterolysis of the O–O bond of the ferric hydroperoxo complex $[(\text{BPMEN})\text{Fe}^{\text{III}}(\text{OOH})]^{2+}$ to form an oxoiron(V) intermediate.²⁸ Our data show that CH_3COOH can also promote the heterolysis of the O–O bond of the ferric alkylperoxo complex $[(\text{BPMEN})\text{Fe}^{\text{III}}(\text{OO}^t\text{Bu})]^{2+}$.

The Systems $2/\text{H}_2\text{O}_2$ and $2/\text{H}_2\text{O}_2/\text{CH}_3\text{COOH}$. The EPR spectrum of the sample 1:2 $2/\text{H}_2\text{O}_2$ frozen 20 min after the reaction onset at $-70\text{ }^{\circ}\text{C}$ in a 1.7:1 $\text{CH}_2\text{Cl}_2/\text{CH}_3\text{CN}$ mixture displays, predominantly, resonances of the hydroperoxo complex $[(\text{TPA})\text{Fe}^{\text{III}}(\text{OOH})(\text{CH}_3\text{CN})]^{2+}$ ($2a\text{-CH}_3\text{CN}$; Figure 9A,

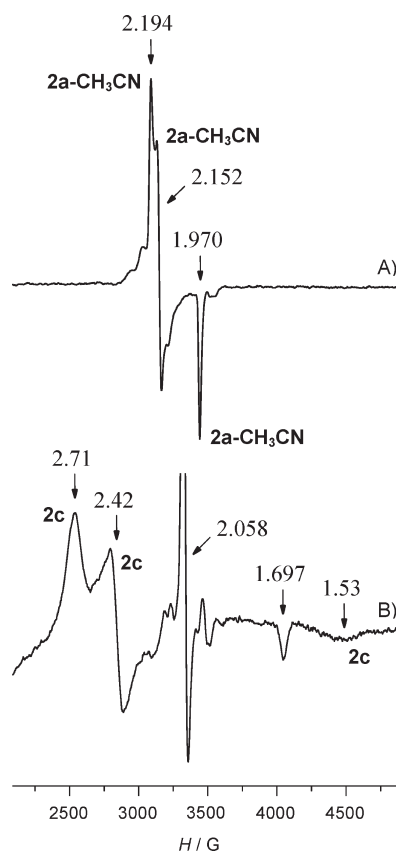


Figure 9. EPR spectrum ($-196\text{ }^{\circ}\text{C}$) of the sample $2/\text{H}_2\text{O}_2$ ($[\text{H}_2\text{O}_2]:[2] = 2$, $[2] = 0.04\text{ M}$) recorded 20 min after mixing the reagents at $-70\text{ }^{\circ}\text{C}$ in a 1.7:1 $\text{CH}_2\text{Cl}_2/\text{CH}_3\text{CN}$ mixture (A). EPR spectrum ($-196\text{ }^{\circ}\text{C}$) of the sample $2/\text{H}_2\text{O}_2/\text{CH}_3\text{COOH}$ ($[2]/[\text{H}_2\text{O}_2]/[\text{CH}_3\text{COOH}] = 1:2:10$, $[2] = 0.04\text{ M}$) recorded 1 min after mixing the reagents at $-60\text{ }^{\circ}\text{C}$ in a 1.7:1 $\text{CH}_2\text{Cl}_2/\text{CH}_3\text{CN}$ mixture (B).

Table 1), in contrast to the system $1/\text{H}_2\text{O}_2$, where resonances of **1a-CH₃CN**, **1a-H₂O**, **1b**, and **1c** were observed (Figures 1 and 2). One can expect that the catalyst system $2/\text{H}_2\text{O}_2$ will be much less selective toward the epoxidation of cyclohexene than the catalyst system $1/\text{H}_2\text{O}_2$, since the former displays no detectable EPR resonances of the active epoxidizing agent analogous to **1c**. In full agreement with this prediction, the system $2/\text{H}_2\text{O}_2$ is a poorer epoxidizing system as compared to the system $1/\text{H}_2\text{O}_2$ (Table 3, entries 1 and 12).

It has been found recently that the addition of acetic acid to the catalyst systems $1/\text{H}_2\text{O}_2$ and $2/\text{H}_2\text{O}_2$ results in an increase in both catalytic activity and selectivity toward the epoxidation of cyclooctene.^{28,53} Similarly, the addition of acetic acid to the catalyst system $2/\text{H}_2\text{O}_2$ noticeably improves its selectivity toward the epoxidation of cyclohexene (compare entries 12 and 13 in Table 3). Interestingly, in contrast to the sample 1:2 $2/\text{H}_2\text{O}_2$ exhibiting EPR resonances of **2a-CH₃CN** (Figure 9A), the EPR spectrum of the sample 1:2:10 $2/\text{H}_2\text{O}_2/\text{CH}_3\text{COOH}$ displays resonances of complex **2c** ($g_1 = 2.71$, $g_2 = 2.42$, $g_3 = 1.53$), which are very similar to those of complex **1c** ($g_1 = 2.69$, $g_2 = 2.42$, $g_3 = 1.70$; Figure 9B). Hence, the increase of epoxidation selectivity of the system $2/\text{H}_2\text{O}_2$ upon the addition of acetic acid correlates with the appearance of the resonances of **2c** in the EPR spectrum. **2c** is very unstable and rapidly disappears even at $-70\text{ }^{\circ}\text{C}$. The maximum concentration of **2c** in the systems 1:2:10 $2/\text{H}_2\text{O}_2/\text{CH}_3\text{COOH}$ and 1:2 $2/$

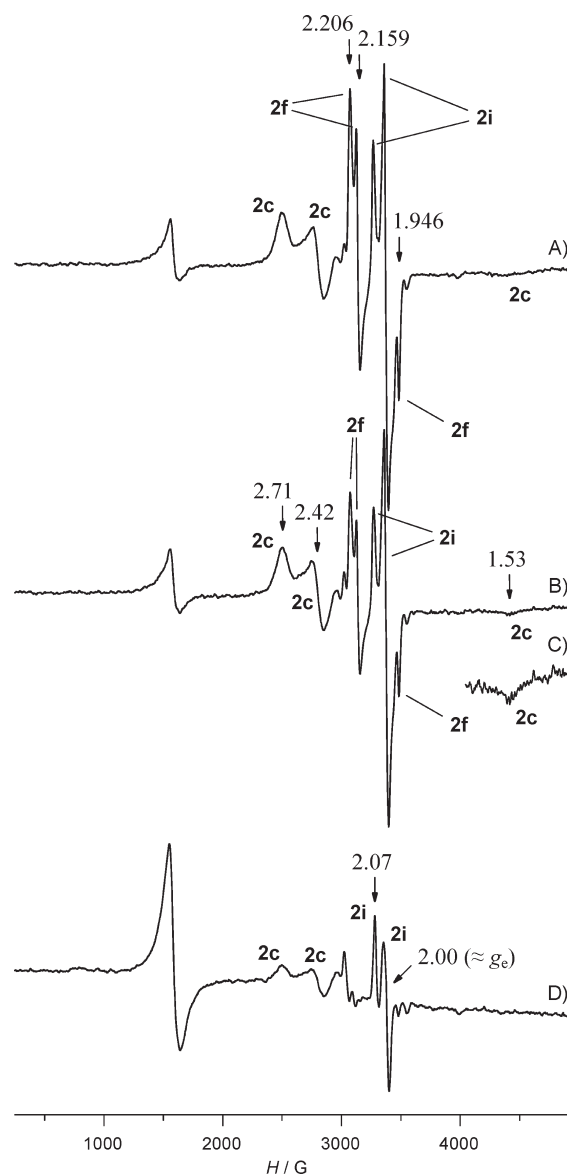


Figure 10. EPR spectra ($-196\text{ }^{\circ}\text{C}$) of the sample $2/\text{CH}_3\text{CO}_3\text{H}$ ($[\text{CH}_3\text{CO}_3\text{H}]/[2] = 2$, $[2] = 0.04\text{ M}$) frozen after mixing the reagents for 30 s at $-60\text{ }^{\circ}\text{C}$ in a 1.7:1 $\text{CH}_2\text{Cl}_2/\text{CH}_3\text{CN}$ mixture and storing it at $-70\text{ }^{\circ}\text{C}$ for 1 min (A), 3 min (B), and 15 min (D). Peak at $g_3 = 1.53$ of the spectrum in "A" at 4 times higher gain (C).

$\text{CH}_3\text{CO}_3\text{H}$ does not exceed 8% of the total iron concentration. More detailed data on the stability and reactivity of **2c** will be presented below. Besides resonances of complex **2c**, the EPR spectrum of Figure 9B displays a relatively sharp spectrum at $g_1 = g_2 = 2.058$ and $g_3 = 1.697$ from an unidentified ferric complex. This complex can be observed even upon storing the sample at $20\text{ }^{\circ}\text{C}$ and thus is of little interest for mechanistic studies.

The Systems $2/\text{CH}_3\text{CO}_3\text{H}$ and $2/m\text{-CPBA}$. The EPR spectra of the sample 1:2 $2/\text{CH}_3\text{CO}_3\text{H}$ frozen at various moments of time after mixing the reagents at $-70\text{ }^{\circ}\text{C}$ show resonances of complexes **2c**, **2f**, and **2i** (Figure 10, Table 1). It is reasonable to expect that the system $2/\text{CH}_3\text{CO}_3\text{H}$ will be a good epoxidizing system, since it generates the proposed epoxidizing agent **2c**. The results of the catalytic studies are in good agreement with this prediction (Table 3, entry 14).

The structures of **2f** and **2i** are still unclear. The EPR spectrum of **2f** is characteristic of low-spin ferric hydroperoxo and alkylperoxo species, but its parameters differ from those for $[(\text{TPA})\text{Fe}^{\text{III}}(\text{OOH})(\text{S})]^{2+}$ and $[(\text{TPA})\text{Fe}^{\text{III}}(\text{OO}^t\text{Bu})(\text{S})]^{2+}$ (Table 1). Moreover, the latter species are stable at -70°C , whereas **2f** decays with $\tau_{1/2} = 5$ min at this temperature. It is tempting to assign **2f** to the low-spin acylperoxo complex $[(\text{TPA})\text{Fe}^{\text{III}}(\text{O}_3\text{CCH}_3)(\text{S})]^{2+}$.

The g values of **2i** ($g_{\perp} \approx g_e$, $g_{\parallel} = 2.07$) closely resemble those for the superoxo heme complexes $(\text{P})\text{Fe}^{\text{II}}(\text{O}_2^{\cdot-})$ ($g_{\perp} \approx g_e$, $g_{\parallel} = 2.11$, P = porphyrin ligand),⁵⁴ and **2i** can be tentatively assigned to the superoxo complex $[(\text{TPA})\text{Fe}^{\text{II}}(\text{O}_2^{\cdot-})(\text{S})]^{+}$. Further studies are needed to verify the proposed structures of **2f** and **2i**.

As in the case of **1**-based systems, the oxoiron(IV) intermediate $[(\text{TPA})\text{Fe}^{\text{IV}}=\text{O}]^{2+}$ (**2d**) can be observed in the system **2**/ $\text{CH}_3\text{CO}_3\text{H}$ with ^1H NMR.³³ Previously, this intermediate was reliably characterized by various spectroscopic techniques, and its reactivity toward various substrates was studied.^{28,30,34} Note that **2d** displays poor epoxidation selectivity, like oxoiron(IV) complex **1d**.²⁸ In contrast to the system **1**/ $\text{CD}_3\text{CO}_3\text{H}$, the high-spin intermediate of the type $[(\text{TPA})\text{Fe}^{\text{III}}(\text{O}_3\text{CCD}_3)]^{2+}$ or $[(\text{TPA})\text{Fe}^{\text{III}}(\text{OOCDD}_3)]^{2+}$ was not observed in the system **2**/ $\text{CD}_3\text{CO}_3\text{H}$ using ^2H NMR. This can be caused by the stronger tendency of TPA-based ferric species to adopt the low-spin state.

Similar to **1c**, complex **2c** is the most likely candidate for the role of the active species of epoxidation. The EPR spectra (-196°C) of a sample frozen after mixing **2** with *m*-CPBA (2 equiv) at -60°C for 30 s and storing it at -70°C show predominantly signals of **2c** (Figure S1, Supporting Information). The simulated spectrum of **2c** is in excellent agreement with the experimental one (Figure S2, Supporting Information). The maximum concentration of **2c** amounts to 15% of the total iron concentration. Self-decay of **2c** follows first-order kinetics with an apparent rate constant of $(1.6 \pm 0.2) \times 10^{-3} \text{ s}^{-1}$ at -70°C . The rate of this decay increases by a factor of 2.5 in the presence of 6 equiv of cyclohexene, by a factor of 5 in the presence of 12 equiv of cyclohexene, and by a factor of 7 in the presence of 18 equiv of cyclohexene, thus indicating that **2c** is reactive toward cyclohexene oxidation even at -70°C (compare Figures S1 and S3 in the Supporting Information). The predominant reaction product formed 1 h after mixing the reagents in the sample 1:2:40 **2**/*m*-CPBA/ C_6H_{10} at -70°C is cyclohexene oxide (yield 84% toward **2**, Table 2, entry 6).⁵⁵ The presented data suggest that the reaction of **2c** with cyclohexene at -70°C leads to cyclohexene oxide. The decay rate of **2c** at -70°C increases by a factor of 4 in the presence of 12 equiv of 1-hexene or 1-octene and does not substantially change upon the addition of 12 equiv of electron-deficient olefins, such as 2-cyclohexene-1-one, 1-acetyl-1-cyclohexene, and cyclohexene-1-carbonitrile.⁵⁷ This is consistent with the presumed electrophilic nature of **2c**.

The Systems 2^tBuOOH and $2^t\text{BuOOH}/\text{CH}_3\text{COOH}$. The catalyst system 2^tBuOOH , as well as the catalyst system 1^tBuOOH , is not able to epoxidize cyclohexene (Table 3, entries 15 and 18). Thus, one can expect that the system 2^tBuOOH will display no resonances of the epoxidizing species **2c**. Indeed, EPR spectra of the system 2^tBuOOH recorded under conditions suitable for the detection of **2c** display only resonances of the alkylperoxo complex $[(\text{TPA})\text{Fe}^{\text{III}}(\text{OO}^t\text{Bu})(\text{CH}_3\text{CN})]^{2+}$ (**2g-CH₃CN**; Figure 11A, Table 1).

As was shown above, the system **1**/ $^t\text{BuOOH}/\text{CH}_3\text{COOH}$ displays the EPR resonances of the epoxidizing agent **1c** (Figure 8) and can epoxidize cyclohexene (Table 3, entries 5,

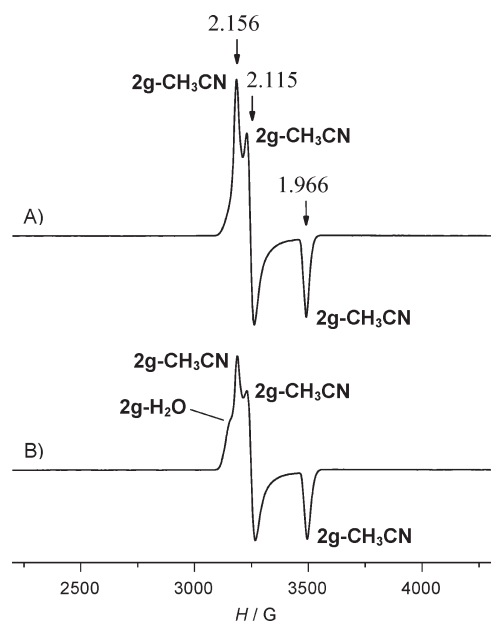


Figure 11. EPR spectrum (-196°C) of the sample 2^tBuOOH ($[^t\text{BuOOH}]/[\mathbf{2}] = 2.5$, $[\mathbf{2}] = 0.05 \text{ M}$) frozen 30 s after mixing the reagents at -60°C in a 1.5:1 $\text{CH}_2\text{Cl}_2/\text{CH}_3\text{CN}$ mixture (A). EPR spectrum (-196°C) of the sample $2^t\text{BuOOH}/\text{CH}_3\text{COOH}$ ($[\mathbf{2}]/[^t\text{BuOOH}]/[\text{CH}_3\text{COOH}] = 1:2.5:10$, $[\mathbf{2}] = 0.05 \text{ M}$) frozen 1 min after mixing the reagents at -60°C in a 1.5:1 $\text{CH}_2\text{Cl}_2/\text{CH}_3\text{CN}$ mixture (B).

6, 8, and 9). In contrast, the system $2^t\text{BuOOH}/\text{CH}_3\text{COOH}$ is inert in this reaction (Table 3, entries 16, 17, 19, and 20). Thus, one can predict that the system $2^t\text{BuOOH}/\text{CH}_3\text{COOH}$ will display no resonances of the epoxidizing agent **2c**. In agreement with this prediction, the EPR spectra of the system $2^t\text{BuOOH}/\text{CH}_3\text{COOH}$ recorded in various moments of time after the reaction onset at -60°C display the resonances of the alkylperoxo complexes **2g-CH₃CN** and **2g-H₂O** (Figure 11B).

The analysis of the EPR and catalytic data for the systems based on complexes **1** and **2** and various oxidants shows that the only systems displaying EPR resonances of the intermediates **1c** and **2c** can drive the selective epoxidation of cyclohexene (**1**/ H_2O_2 , **1**(**2**)/ $\text{H}_2\text{O}_2/\text{CH}_3\text{COOH}$, **1**(**2**)/ $\text{CH}_3\text{CO}_3\text{H}$, **1**(**2**)/*m*-CPBA, and **1**/ $^t\text{BuOOH}/\text{CH}_3\text{COOH}$), whereas the systems exhibiting no EPR resonances of **1c** and **2c** are poor epoxidizing systems (**2**/ H_2O_2 , **1**(**2**)/PhIO, **1**(**2**)/ $^t\text{BuOOH}$, and $2^t\text{BuOOH}/\text{CH}_3\text{COOH}$). Hence, for both complexes **1** and **2**, the epoxidation activity strongly correlates with the formation of the intermediates **1c** and **2c** in the catalyst system. These data are in good agreement with the proposed key role of these intermediates in selective epoxidation.

Possible Nature of the Epoxidizing Agents **1c and **2c**.** The intermediates **1c** and **2c** display the EPR spectra characteristic of $S = 1/2$ species. EPR spectra with close parameters were previously observed for the low-spin ferric complexes with heme ligand tetraphenylporphyrin (TPP, Table 1).¹ However, these ferric complexes contain no active oxygen and thus cannot be considered as potential structural models for **1c** and **2c**.

The EPR spectra of the low-spin species $[(\text{L})\text{Fe}^{\text{III}}(\text{OOR})(\text{S})]^{2+}$ (L = TPA or BPMEN, R = H or ^tBu) are sensitive to the nature of R (Table 1), whereas the same complex **1c** is observed in the systems **1**/ H_2O_2 , **1**/ $\text{CH}_3\text{CO}_3\text{H}$, **1**/ $^t\text{BuOOH}/\text{CH}_3\text{COOH}$, and **1**/*m*-CPBA. The insensitivity of the EPR parameters of **1c** to

suggesting that the reaction of **1c** and cyclohexene leads to the formation of cyclohexene oxide and, most probably, hydroxo complex **1b**. All iron–oxygen species depicted in Scheme 1 can be observed by EPR spectroscopy in the system **1**/ H_2O_2 (Figures 1 and 2). In the catalyst systems **1**/ H_2O_2 / CH_3COOH and **1**/ $t\text{BuOOH}$ / CH_3COOH , the epoxidizing agent **1c** is proposed to derive from the acetic-acid-assisted heterolysis of the O–O bond of the iron(III)-hydroperoxo or iron(III)-alkylperoxo species (Scheme 2a).²⁸ In the peracid-based systems **1**/ $\text{CH}_3\text{CO}_3\text{H}$ and **1**/*m*-CPBA, **1c** is probably generated from the O–O bond heterolysis of iron(III)-acylperoxo complexes (Scheme 2b).⁴⁸ Peracetic acid used in this study contains a great amount of CH_3COOH . Thus, in the system **1**/ $\text{CH}_3\text{CO}_3\text{H}$, **1c** can also originate from the acetic-acid-assisted pathway (Scheme 2a, $\text{R} = \text{C}(\text{O})\text{CH}_3$).

It is of note that the epoxidation activities of the catalyst systems **1**/ H_2O_2 (2.8%) and **1**/ $\text{CH}_3\text{CO}_3\text{H}$ (77%) at -70°C are strictly different (Table 2, entries 1 and 3). In accordance with the mechanistic landscape suggested by Que et al.,²⁸ we assume that the putative intermediates $(\text{BPMEN})\text{Fe}^{\text{V}}=\text{O}$ (**1c**) formed in the systems **1**/ H_2O_2 and **1**/ $\text{CH}_3\text{CO}_3\text{H}$ possess different sixth ligands (HO^- and AcO^- , Schemes 1 and 2b, respectively) and thus display different activities in the epoxidation of cyclohexene at -70°C .

CONCLUSIONS

Through the use of EPR and ^1H and ^2H NMR spectroscopy and conducting reactivity studies, the capability of unstable iron–oxygen intermediates formed in the catalyst systems **1**(**2**)/ H_2O_2 , **1**(**2**)/ H_2O_2 / CH_3COOH , **1**(**2**)/ $\text{CH}_3\text{CO}_3\text{H}$, **1**(**2**)/*m*-CPBA, **1**(**2**)/PhIO, **1**(**2**)/ $t\text{BuOOH}$, and **1**(**2**)/ $t\text{BuOOH}$ / CH_3COOH to conduct olefin epoxidation was elucidated. On the basis of the systematic study, oxoiron(IV) complexes $[(\text{L})\text{Fe}^{\text{IV}}=\text{O}(\text{S})]^{2+}$ and complexes $[(\text{L})\text{Fe}^{\text{III}}(\text{OOR})(\text{S})]^{2+}$ ($\text{R} = \text{H}$ or $t\text{Bu}$) have been shown to be poor epoxidizing agents and thus can be ruled out as the reactive intermediates. In contrast, the highly reactive intermediates **1c** and **2c** with tentative structure $\text{LFe}^{\text{V}}=\text{O}$ ($\text{L} = \text{BPMEN}$ or TPA) have been found to be capable of selectively epoxidizing olefins and hence are the most likely oxygen-transferring agents of the catalyst systems studied. In agreement with this conclusion, only the systems **1**/ H_2O_2 , **1**(**2**)/ H_2O_2 / CH_3COOH , **1**(**2**)/ $\text{CH}_3\text{CO}_3\text{H}$, **1**(**2**)/*m*-CPBA, and **1**/ $t\text{BuOOH}$ / CH_3COOH , displaying EPR spectra of **1c** and **2c**, can epoxidize cyclohexene, whereas the systems **2**/ H_2O_2 , **1**(**2**)/PhIO, **1**(**2**)/ $t\text{BuOOH}$, and **2**/ $t\text{BuOOH}$ / CH_3COOH , exhibiting no EPR resonances of these intermediates, are not able to selectively epoxidize olefins.

The catalyst system **1**/ $t\text{BuOOH}$ / CH_3COOH is a rare example of the nonheme iron-based system capable of selective olefin epoxidation with $t\text{BuOOH}$. The addition of CH_3COOH was found to promote the conversion of $[(\text{BPMEN})\text{Fe}^{\text{III}}(\text{OO}^t\text{Bu})]^{2+}$ to the reactive intermediate **1c**.

EXPERIMENTAL SECTION

Materials. All chemicals and solvents were purchased from Aldrich, Acros Organics, or Alfa Aesar and were used without additional purification unless noted otherwise. Hydrogen peroxide ($\approx 95\%$) was obtained through the concentration of commercial 30% H_2O_2 under reduced pressure. Peroxyacetic acid ($\text{CH}_3\text{CO}_3\text{H}$ or $\text{CD}_3\text{CO}_3\text{H}$) was prepared by mixing equivalent amounts of concentrated H_2O_2 and acetic

acid (CH_3COOH or CD_3COOD) in the presence of 1% H_2SO_4 and stirring the mixture overnight. The exact oxidant contents in the purchased or prepared reagents were determined by iodometric titration under argon. Iodosylbenzene (PhIO) was prepared from diacetoxyiodobenzene as described.⁷¹ Cyclohexene was purified by distilling over sodium metal. Iron complexes $[(\text{BPMEN})\text{Fe}^{\text{II}}(\text{CH}_3\text{CN})_2](\text{ClO}_4)_2$ (**1**) and $[(\text{TPA})\text{Fe}^{\text{II}}(\text{CH}_3\text{CN})_2](\text{ClO}_4)_2$ (**2**) were prepared by a modified procedure.^{51,72}

Caution! Perchlorate salts and concentrated hydrogen peroxide are potentially explosive and should be handled with care.

Instrumentation. ^1H and ^2H NMR spectra were measured in 5 mm cylindrical glass tubes on a Bruker DPX-250 NMR spectrometer at 250.13 MHz and Bruker Avance 400 NMR spectrometer at 61.422 MHz, respectively. Chemical shifts were referenced to the residual peak of the solvent (CHD_2CN or $\text{CD}_2\text{H}_2\text{CN}$, $\delta = 1.96$). To evaluate the concentration of the oxoiron(IV) complex **1d** by ^1H NMR, the integral intensity of the $\text{N}-\text{CH}_3$ peak of **1d** was compared with the integral intensity of the peak of hexamethyldisiloxane added to the solution before the onset of the reaction. Typical operation conditions for ^1H NMR measurements were as follows: spectral width 50 kHz, spectrum accumulation frequency 5 Hz, number of scans 512–1024, radio frequency pulse 5 μs . Typical operation conditions for ^2H NMR measurements were as follows: spectral width 100 kHz, spectrum accumulation frequency 5 Hz, number of scans 5000–10000, radio frequency pulse 10 μs . EPR spectra (-196°C) were measured in 3 mm quartz tubes on a Bruker ER-200D spectrometer at 9.3–9.4 GHz, modulation frequency 100 kHz, modulation amplitude 5 G. The dual EPR cavity furnished with the spectrometer was used. A periclase crystal (MgO) with impurities of Mn^{2+} and Cr^{3+} , which served as a side reference, was placed into the second compartment of the dual cavity. Measurements were conducted in a quartz finger Dewar filled with liquid nitrogen. EPR signals were quantified by double integration with a frozen solution of copper(II) acetylacetonate as a standard at -196°C . EPR spectra were simulated using an extended version of the program ESR1.⁷³ Analyses of cyclohexene oxidation products were performed on an Agilent 6890N gas chromatograph (DB-WAX column, 30 m) with a flame-ionization detector.

Sample Preparation for EPR Measurements. Using a micropipet connected with polyethylene capillary, an appropriate amount of the oxidant in 0.05 mL of CH_3CN was added to 0.35 mL of a solution of iron(II) complex in a CH_2Cl_2 / CH_3CN mixture at -70 to -40°C directly in a quartz EPR tube ($d = 3$ mm). After stirring for 30–60 s with polyethylene capillary at -70 to -40°C , the sample was frozen by immersion in liquid nitrogen, and the EPR spectrum was measured at -196°C . For kinetic EPR studies, this sample was placed in a thermostat at the required temperature directly in the EPR tube. To stop the reaction, the tube was again immersed in liquid nitrogen, followed by registration of the EPR spectrum at -196°C . To measure the reactivity of iron–oxygen intermediates toward olefin epoxidation, an olefin substrate was added to the initial solution of the iron(II) complex.

Sample Preparation for NMR Measurements. Using a micropipet connected with polyethylene capillary, an appropriate amount of the oxidant in 0.1 mL of CD_3CN (or CH_3CN) was added to 0.5 mL of a solution of the iron(II) complex in a CD_2Cl_2 / CD_3CN (or CH_2Cl_2 / CH_3CN) mixture at -50 to 0°C directly in a glass NMR tube ($d = 5$ mm). After stirring for several minutes with a polyethylene capillary at -50 to 0°C , the sample was cooled by immersion in liquid nitrogen for a few seconds and immediately placed in the NMR spectrometer. For kinetic NMR measurements, NMR spectra were recorded at the selected temperature (-50 or -70°C). To measure the reactivity of oxoiron(IV) complex **1d** toward the oxidation of cyclohexene, the appropriate amount of cyclohexene was added to the sample placed in a thermostat at -50 or -70°C after the generation of **1d**.

Reaction Conditions for Catalytic Oxidations at 25°C . In a typical reaction, 0.1 mL of a 0.32 M solution of the oxidant in CH_3CN

(except PhIO) was delivered by syringe pump over 25 min to a vigorously stirred CH₃CN solution (1.1 mL) containing the iron(II) complex and cyclohexene (if necessary, acetic acid was added before the onset of the reaction). The solution was stirred for another 5 min after syringe pump addition was complete. PhIO was added all at once, followed by stirring for 30 min. The final reagent concentrations were as follows: 2.7×10^{-3} M iron(II) complex, 0.027 M oxidant, 0.81 M cyclohexene. The internal standard (1,4-dioxane) was added, and the solution was subjected to GC analysis. The products were identified by comparison of their GC retention times with those of authentic compounds. All reactions were run at least in duplicate, the reported yields being the average of these reactions.

Reaction Conditions for Catalytic Oxidations at -70°C .

For catalytic cyclohexene oxidation with H₂O₂ or CH₃CO₃H, 0.1 mL of a 3.2 M oxidant solution cooled to -70°C was added to the vigorously stirred solution (1.1 mL) containing iron(II) complex, cyclohexene, and the inert internal standard (1,4-dioxane). A 1.3:1 CH₂Cl₂/CH₃CN mixture was used as a solvent. The final reagent concentrations were as follows: 0.027 M iron(II) complex, 0.27 M oxidant, and 0.81 M cyclohexene. After stirring for 1 h, 0.3 mL of a 2.5 M triphenylphosphine solution in CH₂Cl₂ cooled to -70°C was added. The resulting mixture was carefully warmed to room temperature and subjected to GC analysis. The catalytic reactions were run in triplicate. For catalytic cyclohexene oxidation with *m*-CPBA, solid *m*-CPBA (0.048 mmol) cooled to -70°C was added to the vigorously stirred solution (1.2 mL) containing the iron(II) complex, cyclohexene, and the inert internal standard (1,4-dioxane). A 1.3:1 CH₂Cl₂/CH₃CN mixture was used as a solvent. The final reagent concentrations were as follows: 0.02 M iron(II) complex, 0.04 M *m*-CPBA, and 0.8 M cyclohexene. After stirring for 1 h, 0.3 mL of a 2.5 M triphenylphosphine solution in CH₂Cl₂ cooled to -70°C was added. The resulting mixture was carefully warmed to room temperature and subjected to GC analysis. The reactions were run in triplicate. Oxidants utilized (H₂O₂, CH₃CO₃H, and *m*-CPBA) do not oxidize cyclohexene at -70°C in the absence of the iron complex.

■ ASSOCIATED CONTENT

S Supporting Information. ¹H NMR chemical shifts for oxoiron(IV) complex **1d**, simulated and experimental EPR spectra of species **2c**, and EPR monitoring of the interaction of complex **2** with *m*-CPBA. This material is available free of charge via the Internet at <http://pubs.acs.org>.

■ AUTHOR INFORMATION

Corresponding Author

*Fax: +7 383 3308056. E-mail: talsi@catalysis.ru.

■ ACKNOWLEDGMENT

The authors thank the Russian Foundation for Basic Research, Grant 09-03-00087, for financial support.

■ REFERENCES

- (1) Solomon, E. I.; Brunold, T. C.; Davis, M. I.; Kemsley, J. N.; Lee, S.-K.; Lehnert, N.; Neese, F.; Skulan, A. J.; Yang, Y.-S.; Zhou, J. *Chem. Rev.* **2000**, *100*, 235–349.
- (2) Costas, M.; Mehn, M. P.; Jensen, M. P.; Que, L., Jr. *Chem. Rev.* **2004**, *104*, 939–986.
- (3) Tshuva, E. Y.; Lippard, S. J. *Chem. Rev.* **2004**, *104*, 987–1012.
- (4) Kryatov, S. V.; Rybak-Akimova, E. V.; Schindler, S. *Chem. Rev.* **2005**, *105*, 2175–2226.
- (5) Oldenburg, P. D.; Que, L., Jr. *Catal. Today* **2006**, *117*, 15–21.

- (6) Nam, W. *Acc. Chem. Res.* **2007**, *40*, 522–531.
- (7) Que, L., Jr. *Acc. Chem. Res.* **2007**, *40*, 493–500.
- (8) Que, L., Jr.; Tolman, W. B. *Nature* **2008**, *455*, 333–340.
- (9) Bruijninx, P. C. A.; van Koten, G.; Klein Gebbink, R. J. M. *Chem. Soc. Rev.* **2008**, *37*, 2716–2744.
- (10) White, M. C.; Doyle, A. G.; Jacobsen, E. N. *J. Am. Chem. Soc.* **2001**, *123*, 7194–7195.
- (11) Chen, K.; Costas, M.; Kim, J.; Tipton, A. K.; Que, L., Jr. *J. Am. Chem. Soc.* **2002**, *124*, 3026–3035.
- (12) Oldenburg, P. D.; Shteinman, A. A.; Que, L., Jr. *J. Am. Chem. Soc.* **2005**, *127*, 15672–15673.
- (13) England, J.; Britovsek, G. J. P.; Rabadia, N.; White, A. J. P. *Inorg. Chem.* **2007**, *46*, 3752–3767.
- (14) Chen, M. S.; White, M. C. *Science* **2007**, *318*, 783–787.
- (15) England, J.; Davies, C. R.; Banaru, M.; White, A. J. P.; Britovsek, G. J. P. *Adv. Synth. Catal.* **2008**, *350*, 883–897.
- (16) Suzuki, K.; Oldenburg, P. D.; Que, L., Jr. *Angew. Chem., Int. Ed.* **2008**, *47*, 1887–1889.
- (17) Sorokin, A. B.; Kudrik, E. V.; Bouchu, D. *Chem. Commun.* **2008**, 2562–2564.
- (18) Company, A.; Gómez, L.; Fontrodona, X.; Ribas, X.; Costas, M. *Chem.—Eur. J.* **2008**, *14*, 5727–5731.
- (19) Yoon, J.; Wilson, S. A.; Jang, Y. K.; Seo, M. S.; Nehru, K.; Hedman, B.; Hodgson, K. O.; Bill, E.; Solomon, E. I.; Nam, W. *Angew. Chem., Int. Ed.* **2009**, *48*, 1257–1260.
- (20) Schröder, K.; Enthaler, S.; Bitterlich, B.; Schulz, T.; Spannenberg, A.; Tse, M. K.; Junge, K.; Beller, M. *Chem.—Eur. J.* **2009**, *15*, 5471–5481.
- (21) Gómez, L.; Garcia-Bosch, I.; Company, A.; Benet-Buchholz, J.; Polo, A.; Sala, X.; Ribas, X.; Costas, M. *Angew. Chem., Int. Ed.* **2009**, *48*, 5720–5723.
- (22) Lee, S. H.; Han, J. H.; Kwak, H.; Lee, S. J.; Lee, E. Y.; Kim, H. J.; Lee, J. H.; Bae, C.; Lee, S. N.; Kim, Y.; Kim, C. *Chem.—Eur. J.* **2007**, *13*, 9393–9398.
- (23) Gelalcha, F. G.; Anilkumar, G.; Tse, M. K.; Brückner, A.; Beller, M. *Chem.—Eur. J.* **2008**, *14*, 7687–7698.
- (24) Chen, M. S.; White, M. C. *Science* **2010**, *327*, 566–571.
- (25) Möller, K.; Wienhöfer, G.; Schröder, K.; Join, B.; Junge, K.; Beller, M. *Chem.—Eur. J.* **2010**, *16*, 10300–10303.
- (26) Das, P.; Que, L., Jr. *Inorg. Chem.* **2010**, *49*, 9479–9485.
- (27) Makhlynets, O. V.; Rybak-Akimova, E. V. *Chem.—Eur. J.* **2010**, *16*, 13995–14006.
- (28) Mas-Ballester, R.; Que, L., Jr. *J. Am. Chem. Soc.* **2007**, *129*, 15964–15972.
- (29) Kim, C.; Chen, K.; Kim, J.; Que, L., Jr. *J. Am. Chem. Soc.* **1997**, *119*, 5964–5965.
- (30) Lim, M. H.; Rohde, J.-U.; Stubna, A.; Bukowski, M. R.; Costas, M.; Ho, R. Y. N.; Münck, E.; Nam, W.; Que, L., Jr. *Proc. Natl. Acad. Sci. U.S.A.* **2003**, *100*, 3665–3670.
- (31) Lobanova, M. V.; Bryliakov, K. P.; Duban, E. A.; Talsi, E. P. *Mendeleev Commun.* **2003**, 175–177.
- (32) Duban, E. A.; Bryliakov, K. P.; Talsi, E. P. *Mendeleev Commun.* **2005**, 12–14.
- (33) Duban, E. A.; Bryliakov, K. P.; Talsi, E. P. *Eur. J. Inorg. Chem.* **2007**, 852–857.
- (34) Park, M. J.; Lee, J.; Suh, Y.; Kim, J.; Nam, W. *J. Am. Chem. Soc.* **2006**, *128*, 2630–2634.
- (35) de Oliveira, F. T.; Chanda, A.; Banerjee, D.; Shan, X.; Mondal, S.; Que, L., Jr.; Bominaar, E. L.; Münck, E.; Collins, T. J. *Science* **2007**, *315*, 835–838.
- (36) Lyakin, O. Y.; Bryliakov, K. P.; Britovsek, G. J. P.; Talsi, E. P. *J. Am. Chem. Soc.* **2009**, *131*, 10798–10799.
- (37) Some results described in this paper were partially presented in our short communication (see ref 36).
- (38) Seo, M. S.; Kamachi, T.; Kouno, T.; Murata, K.; Park, M. J.; Yoshizawa, K.; Nam, W. *Angew. Chem., Int. Ed.* **2007**, *46*, 2291–2294.
- (39) Duellund, L.; Hazell, R.; McKenzie, C. J.; Nielsen, L. P.; Toftlund, H. *J. Chem. Soc., Dalton Trans.* **2001**, 152–156.

- (40) Roelfes, G.; Lubben, M.; Chen, K.; Ho, R. Y. N.; Meetsma, A.; Genseberger, S.; Hermant, R. M.; Hage, R.; Mandal, S. K.; Young, V. G., Jr.; Zang, Y.; Kooijman, H.; Spek, A. L.; Que, L., Jr.; Feringa, B. L. *Inorg. Chem.* **1999**, *38*, 1929–1936.
- (41) Sugiura, Y. *J. Am. Chem. Soc.* **1980**, *102*, 5208–5215.
- (42) Burger, R. M.; Peisach, J.; Band Horwitz, S. *J. Biol. Chem.* **1981**, *256*, 11636–11644.
- (43) Chen, K.; Costas, M.; Que, L., Jr. *J. Chem. Soc., Dalton Trans.* **2002**, 672–679.
- (44) Chen, K.; Que, L., Jr. *J. Am. Chem. Soc.* **2001**, *123*, 6327–6337.
- (45) Klinker, E. J.; Kaizer, J.; Brennessel, W. W.; Woodrum, N. L.; Cramer, C. J.; Que, L., Jr. *Angew. Chem., Int. Ed.* **2005**, *44*, 3690–3694.
- (46) Britovsek, G. J. P.; England, J.; White, A. J. P. *Inorg. Chem.* **2005**, *44*, 8125–8134.
- (47) England, J.; Gondhia, R.; Bigorra-Lopez, L.; Petersen, A. R.; White, A. J. P.; Britovsek, G. J. P. *Dalton Trans.* **2009**, 5319–5334.
- (48) Oh, N. Y.; Seo, M. S.; Lim, M. H.; Consugar, M. B.; Park, M. J.; Rohde, J.-U.; Han, J.; Kim, K. M.; Kim, J.; Que, L., Jr.; Nam, W. *Chem. Commun.* **2005**, 5644–5646.
- (49) Arasasingham, R. D.; Balch, A. L.; Cornman, C. R.; Latos-Grazynski, L. *J. Am. Chem. Soc.* **1989**, *111*, 4357–4363.
- (50) Kim, J.; Larka, E.; Wilkinson, E. C.; Que, L., Jr. *Angew. Chem., Int. Ed.* **1995**, *34*, 2048–2051.
- (51) Zang, Y.; Kim, J.; Dong, Y.; Wilkinson, E. C.; Appelman, E. H.; Que, L., Jr. *J. Am. Chem. Soc.* **1997**, *119*, 4197–4205.
- (52) Kim, J.; Harrison, R. G.; Kim, C.; Que, L., Jr. *J. Am. Chem. Soc.* **1996**, *118*, 4373–4379.
- (53) Mas-Ballesté, R.; Fujita, M.; Hemmilla, C.; Que, L., Jr. *J. Mol. Catal. A: Chem.* **2006**, *251*, 49–53.
- (54) Davydov, R.; Satterlee, J. D.; Fujii, H.; Sauer-Masarwa, A.; Busch, D. H.; Hoffman, B. M. *J. Am. Chem. Soc.* **2003**, *125*, 16340–16346.
- (55) For the systems **1**(2)/*m*-CPBA/cyclohexene, only a small amount of *m*-CPBA was used (2 equiv relative to **1** or **2**), since these systems are rapidly deactivated via the formation of stable iron(III)–salicylate complexes (products of *ortho*-hydroxylation), which prevents the generation of active species **1c** and **2c**, i.e., the possibility of catalytic turnover (see refs 48 and 56).
- (56) Taktak, S.; Flook, M.; Foxman, B. M.; Que, L., Jr.; Rybak-Akimova, E. V. *Chem. Commun.* **2005**, 5301–5303.
- (57) The experimental conditions are identical to those used in the experiment with the system **2**/*m*-CPBA/cyclohexene = 1:2:12 (see the caption of Figure S3 in the Supporting Information).
- (58) Lacy, D. C.; Gupta, R.; Stone, K. L.; Greaves, J.; Ziller, J. W.; Hendrich, M. P.; Borovik, A. S. *J. Am. Chem. Soc.* **2010**, *132*, 12188–12190.
- (59) Groves, J. T.; Watanabe, Y. *J. Am. Chem. Soc.* **1988**, *110*, 8443–8452.
- (60) Soper, J. D.; Kryatov, S. V.; Rybak-Akimova, E. V.; Nocera, D. G. *J. Am. Chem. Soc.* **2007**, *129*, 5069–5075.
- (61) Ambrozich, D. L.; Saburi, M.; Fendler, J. H. *J. Am. Chem. Soc.* **1980**, *102*, 6374–6375.
- (62) Hill, C. L.; Schardt, B. C. *J. Am. Chem. Soc.* **1980**, *102*, 6375–6377.
- (63) Groves, J. T.; Lee, J.; Marla, S. S. *J. Am. Chem. Soc.* **1997**, *119*, 6269–6273.
- (64) Nam, W.; Kim, I.; Lim, M. H.; Choi, H. J.; Lee, J. S.; Jang, H. G. *Chem.—Eur. J.* **2002**, *8*, 2067–2071.
- (65) Bryliakov, K. P.; Babushkin, D. E.; Talsi, E. P. *J. Mol. Catal. A: Chem.* **2000**, *158*, 19–35.
- (66) Schappacher, M.; Weiss, R. *Inorg. Chem.* **1987**, *26*, 1189–1190.
- (67) Ottenbacher, R. V.; Bryliakov, K. P.; Talsi, E. P. *Inorg. Chem.* **2010**, *49*, 8620–8628.
- (68) Grapperhaus, C. A.; Mienert, B.; Bill, E.; Weyhermüller, T.; Wieghardt, K. *Inorg. Chem.* **2000**, *39*, 5306–5317.
- (69) Rohde, J.-U.; In, J.-H.; Lim, M. H.; Brennessel, W. W.; Bukowski, M. R.; Stubna, A.; Münck, E.; Nam, W.; Que, L., Jr. *Science* **2003**, *299*, 1037–1039.
- (70) Bolland, V.; Charlot, M.-F.; Banse, F.; Girerd, J.-J.; Mattioli, T. A.; Bill, E.; Bartoli, J.-F.; Battioni, P.; Mansuy, D. *Eur. J. Inorg. Chem.* **2004**, 301–308.
- (71) Piaggio, P.; McMorn, P.; Murphy, D.; Bethell, D.; Bulman Page, P. C.; Hancock, F. E.; Sly, C.; Kerton, O. J.; Hutchings, G. I. *Chem. Soc., Perkin Trans. 2* **2000**, 2008–2015.
- (72) Chen, K.; Que, L., Jr. *Chem. Commun.* **1999**, 1375–1376.
- (73) Shubin, A. A.; Zhidomirov, G. M. *J. Struct. Chem.* **1989**, *30*, 414–417.